

Accepted Manuscript

International Journal of Structural Stability and Dynamics

Article Title: Local mass addition and data fusion for structural damage identification using approximate models

Author(s): Jilin Hou, Zhenkun Li, Qingxia Zhang, Lukasz Jankowski, Haibin Zhang

DOI: 10.1142/S0219455420501242

Received: 08 March 2020

Accepted: 26 July 2020

To be cited as: Jilin Hou *et al.*, Local mass addition and data fusion for structural damage identification using approximate models, *International Journal of Structural Stability and Dynamics*, doi: 10.1142/S0219455420501242

Link to final version: <https://doi.org/10.1142/S0219455420501242>

This is an unedited version of the accepted manuscript scheduled for publication. It has been uploaded in advance for the benefit of our customers. The manuscript will be copyedited, typeset and proofread before it is released in the final form. As a result, the published copy may differ from the unedited version. Readers should obtain the final version from the above link when it is published. The authors are responsible for the content of this Accepted Article.

Local mass addition and data fusion for structural damage identification using approximate models

Jilin Hou^{*††}, Zhenkun Li^{*}, Qingxia Zhang[†], Łukasz Jankowski[§] and Haibin Zhang^{*}

**School of Civil Engineering
State Key Laboratory of Coastal and Offshore Engineering
Dalian University of Technology
Dalian 116023, P. R. China*

*†School of Civil Engineering
Dalian Minzu University, Dalian 116650, P. R. China*

*§Institute of Fundamental Technological Research
Polish Academy of Sciences, 02-106 Warsaw, Poland*

Received

Accepted

Published

In practical civil engineering, structural damage identification is difficult to implement due to the shortage of the measured modal information and the influence of noise. Furthermore, typical damage identification methods generally rely on a precise Finite Element (FE) model of the monitored structure. Pointwise mass alterations of the structure can effectively improve the quantity and sensitivity of measured data, while the data fusion methods can adequately utilize various kinds of data and identification results. This paper proposes a damage identification method that requires only approximate FE models and combines the advantages of pointwise mass additions and data fusion. First, an additional mass is placed at different positions throughout the structure to collect the dynamic response and obtain the corresponding modal information. The resulting relation between natural frequencies and the position of the added mass is sensitive to local damage, and it is thus utilized to form a new objective function based on the modal assurance criterion (MAC) and l_1 -based sparsity promotion. The proposed objective function is mostly insensitive to global structural parameters, but remains sensitive to local damage. Several approximate FE models are then established and separately used to identify the damage of the structure. Finally, the Dempster-Shafer method of data fusion is applied to fuse the results from all the approximate models. Such an approach circumvents the need for a precise FE model, which is usually not easy to obtain in real application, and thus enhances the practical applicability of the proposed method, while maintaining the damage identification accuracy. The proposed approach is verified numerically and experimentally. Numerical simulations of a simply supported beam and a long-span bridge confirm that it can be used for damage identification, including a single damage and multiple damages, with a high accuracy. Finally, an experiment of a cantilever beam is successfully performed.

Keywords: structural health monitoring (SHM), damage identification, adding mass, data fusion, objective function, modal assurance criterion(MAC)

1. INTRODUCTION

Structural health monitoring (SHM) [1], as a frontier technology for assessing structural health, has become a hot topic in modern civil engineering field [2,3]. As the crucial part of a health monitoring system, damage

^{††}Corresponding authors. 1

identification provides a reliable foundation for structural damage assessment 4. Yang et al. 5 comprehensively reviewed state-of-the-art in damage detection methods for bridges by using moving test vehicles. Such instrumented vehicles are used to extract dynamic characteristics of a bridge for the purpose of modal identification and damage detection, without the need to install any vibration sensors on the bridge 6. Wang et al 7 established a complete health monitoring system for damage identification in large structures and used the proposed EOT method to detect single damages of a long span bridge; the results showed that the method can be applied in practical engineering. Maalej et al. 8 used a fiber optics sensing system embedded in a bridge to monitor its health condition in real-time. Structural damage identification methods based directly on the dynamic response have been widely studied due to their simple manipulation process and relatively accurate results. However, there are also persistent difficulties that hinder practical applications: the experimental data are often not enough independent and sensitive to allow a larger number of damage parameters to be accurately identified, and moreover, a FE model cannot be often built precisely enough for parameter optimization.

Physical or virtual alteration of structural parameters has been shown to be an effective way to increase the amount and sensitivity of experimental data. Nalitolela et al. 9 proposed the idea to add masses to the structure or to modify its local stiffness in order to update the related perturbed structural model. Gillichet al. 10 utilized a perfectly clamped-free beam to study the influence of stepwise eccentric distributed masses on the structural modal characteristics and derived analytical formulas to calculate the natural frequencies and mode shapes. Deng et al. 11 obtained the mass-normalized modal shapes by adding external masses to the structure; the method was verified using a steel cantilever beam. Lee and Eun 12 utilized a 2D frame structure model and proposed a damage identification method based on its response variation and additional mass. The damage was identified by the change of the frequency response function (FRF) that occurred due to the additional mass. Zhou et al. 13 established generalized flexibility equations to identify damage parameters by adding determined mass blocks at certain parts of the structure. Based on the preceding methods and analysis, Hou et al. 14 proposed that, instead of physical masses, virtual masses can be added; the addition and analysis of the virtual masses was realized and validated by numerical simulation. A sensitivity analysis of the natural frequencies was performed in order to determine the optimal masses. In general, adding masses to a structure is a relatively straightforward procedure. Natural frequencies are the most fundamental modal parameters of the structure, and by adding properly placed masses, they can be made sensitive to local damage. Therefore, aiming at the problems of the insufficient modal information in practical engineering and its low sensitivity to local damage, this paper uses an additional mass added in various locations to the original structure in order to enhance the amount, quality and sensitivity of experimental data. As a result, more independent information is available and can be used to calculate the unknown damage parameters.

Damage identification methods based on the dynamic response can be generally divided into model-free and model-based methods. Model-free methods do not require a typical parametric structural model: they analyze the structural response either directly or in the form of the estimated structural modal characteristics. These methods include mainly signal processing and dynamic signature approaches. The former (signal processing) rely often on the wavelet transform, empirical mode decomposition (EMD) or variational mode decomposition (VMD). For example, Cao et al. 15 proposed the integrated wavelet transform (IWT), which can be used for effective elimination of the random noise and regular interferences to extract pure damage-related information. Wang et al. 16 utilized the EMD method to decompose the vibration response data of the rod end node into a series of intrinsic mode functions (IMFs), which could reveal the damage status of the structure. Dragomiretskiy et al. 17 proposed a non-recursive VMD model, where the modes are extracted concurrently, and the model is shown to be robust to sampling and noise. The dynamic signature methods are often based on natural frequencies and/or modal shapes. For example, Gillich et al. 18 presented a method based on natural frequency changes before and after the damage. The method was able to detect the damage in beam-like structures and to identify the damage position and extent. Patil et al. 19 used experimental test data to detect multiple cracks in a beam structure based on natural frequencies and utilized a specimen made of aluminum alloy to verify the method. Cao et al. 20 investigated damage identification of a cantilever beam structure based on mode shapes and static deflection. Xu et al. 21 proposed structural damage detection methods based on distributed strain measurement under the influence of ambient noise, in which a numerical example of a long-span cable-stayed bridge is used to verify the accuracy and effectiveness of the proposed technique. The model-free methods avoid the problematic stage of building and updating a FE structural model, but they usually cannot be used for quantitative damage identification and are often sensitive to noise.

The model-based methods rely on a FE structural model. They use the residuals between measured and simulated structural characteristics to establish the objective function, and then they identify structural damages by model updating and optimization methods. West et al.²² validated that MAC can be used for damage identification; in the test, modal models of a bulkhead were constructed before and after environment acoustic tests and compared by computing their MAC to detect significant structural changes. Deng et al.²³ updated a model of a bridge structure to find its damages using the response surface method and a genetic algorithm. Jaishi et al.²⁴ conducted structural damage identification based on model correction and residual modal flexibility. Mekjavić et al.²⁵ employed measured natural frequencies to locate and quantify bridge damages. The proposed direct iteration technique was well verified by a six-span steel girder bridge. Wu et al.²⁶ proposed a model updating method for structural damage identification using l_1 regularization; two criteria (frequencies and a combination of frequencies and mode shapes) were considered and a cantilever beam was utilized to verify experimentally the effectiveness of the proposed method. The model-based methods can quantitatively identify structural damage, but they indispensably require an accurate FE model to be updated. The need for a very accurately updated FE model is often their crucial weakness in real applications, and this is exactly the problem addressed in this paper: if an accurate FE model cannot be obtained in a real application, it is proposed here to (1) form a new objective function that makes use of the increased amount of data obtained in a series of local alterations of structural mass, (2) identify the damage by updating several approximate FE models and performing data fusion of the results.

Data fusion is a relatively new technique for multi-source information synthesis and processing, which can generate reliable and accurate results by combining and exploiting information available from various sources. The algorithms for data fusion include mainly Bayes reasoning²⁷, Dempster-Shafer (D-S) evidence theory^{28,29}, and fuzzy logic³⁰. The D-S evidence theory has recently attracted an increasing amount of interests for its unique advantages of flexibility and simplicity³¹: a systematic introduction can be found in Deng³². Liu et al.³³ proposed two damage identification methods based on multi-source information fusion. He et al.³⁴ used data fusion to carry out health monitoring and damage identification of an Unmanned Aerial Vehicle (UAV) structure and adopted multi-source and multi-attribute data fusion methods to generate accurate results, which were found to be more precise than the results obtained based on a single information source. Vanniamparambil et al.³⁵ used data fusion to accurately quantify the damage of reinforced concrete masonry walls. Based on a heterogeneous data fusion method and Bayesian regularization, Sun et al.³⁶ proposed an effective algorithm that can identify traffic-induced excitations of truss bridges. In practical engineering, the actual structure is usually complex, and a FE model of the required accuracy might not be available, while an inaccurate model can undermine damage identification or significantly decrease its accuracy. Therefore, instead of striving for an accurate FE model, it is proposed here to exploit data fusion techniques as applied to a number of approximate FE models: even if neither of these approximate models can provide accurate identification by itself, it is demonstrated here that the approximate models treated as an ensemble can provide information that, fused together, is accurate enough for reliable identification.

The structure of the paper is as follows: Section 2 introduces the concept of the proposed damage identification method by local mass alterations in the form of sequential mass adding. Section 3 explains the proposed multi-model data fusion in application to damage identification. Section 4 verifies the method numerically by using FE models of a simply supported beam and a continuous long-span bridge. Finally, Section 5 validates the approach experimentally by applying it to a physical cantilever beam.

2. DAMAGE IDENTIFICATION BASED ON ADDING MASSES

The proposed process of mass additions for damage identification is as follows: First, a mass (or potentially more masses) are sequentially added (and then removed) at different positions to the structure, and each time the corresponding structural dynamic measurements are collected. The natural frequencies of the structure (with masses added at different positions) are identified, which yields a relation between the identified natural frequencies and the position of the additional mass. Finally, the MAC is used to establish the objective function, which quantifies the deviation between the experimentally obtained relation and the simulation results. The resulting function is used in Section 3 for model updating purposes with a number of approximate models.

2.1. Adding masses at different positions

When a mass is added to the structure, the structural modal characteristics change. Therefore, by adding masses at different positions, a large number of structural modal parameters can be acquired. Thanks to the local character of the employed pointwise mass addition, the modal characteristics obtained this way are much more sensitive to local damages than the corresponding global characteristics of the original unaltered structure.

As shown in Fig. 1, a number of positions, x_1 to x_k , are first determined throughout the monitored structure. When a mass m is added at the position x_1 , the structural dynamic response measurements are performed to obtain the first n natural frequencies of the structure, which are collected as the vector $\hat{\omega}_1 = [\omega_{1,1}, \omega_{2,1}, \dots, \omega_{n,1}]$. Then the mass m is moved to the next position x_2 to obtain the vector $\hat{\omega}_2 = [\omega_{1,2}, \omega_{2,2}, \dots, \omega_{n,2}]$, and the process is successively continued up to the last position x_k to obtain the vector $\hat{\omega}_k = [\omega_{1,k}, \omega_{2,k}, \dots, \omega_{n,k}]$, where $\omega_{i,j}$ is the i th natural frequency of the monitored structure with the mass attached at the position x_j . Finally, all the frequencies obtained from the experiment are arranged into a single matrix \mathbf{W}_m as follows:

$$\mathbf{W}_m = [\hat{\omega}_1^T, \hat{\omega}_2^T, \dots, \hat{\omega}_k^T]^T. \quad (1)$$

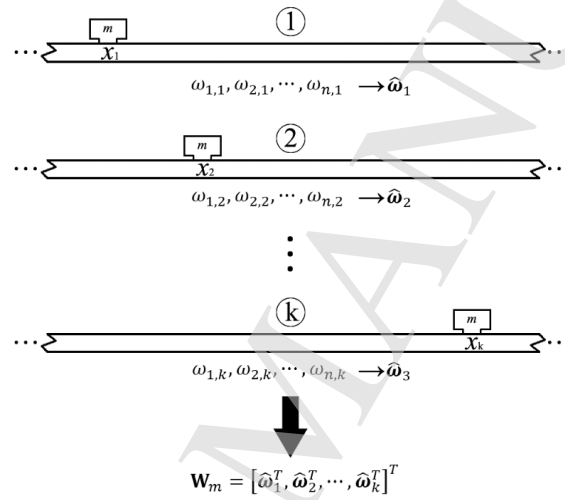


Fig. 1. Adding a mass at different positions of the monitored structure

2.2. The objective function

Model-based damage identification requires a FE model of the intact structure. Let \mathbf{M} and \mathbf{K} denote respectively the mass matrix and the stiffness matrix. The structure is divided into N substructures. Structural damage is modeled as stiffness reduction of the substructures and quantified in terms of the vector $\boldsymbol{\mu} = [\mu_1, \mu_2, \dots, \mu_N]^T$, where μ_i is the ratio of the stiffness of the i th substructure after being damaged to its original stiffness, i.e., the damage factor of the i th substructure. Let \mathbf{K}_i be the stiffness matrix of the i th substructure in the global coordinates. The stiffness matrix $\mathbf{K}_d(\boldsymbol{\mu})$ of the entire damaged structure can be expressed as

$$\mathbf{K}_d(\boldsymbol{\mu}) = \sum_{i=1}^N \mu_i \mathbf{K}_i \quad (2)$$

The proposed mass addition affects the mass matrix of the structure. Let \mathbf{M}_j denote the global mass matrix of the structure with the mass m added at the position x_j . Assumed the damage factor $\boldsymbol{\mu}$ and the position x_j of the added mass, the corresponding vector $\boldsymbol{\omega}_j^F(\boldsymbol{\mu}) = [\omega_{1,j}^F(\boldsymbol{\mu}), \omega_{2,j}^F(\boldsymbol{\mu}), \dots, \omega_{n,j}^F(\boldsymbol{\mu})]$ of the first n natural frequencies can be straightforwardly calculated by using the eigenvalue decomposition of the structural stiffness and mass matrices $\mathbf{K}_d(\boldsymbol{\mu})$ and \mathbf{M}_j . The most straightforward way of comparing the theoretical natural frequencies $\omega_{i,j}^F(\boldsymbol{\mu})$ with the experimentally obtained natural frequencies $\omega_{i,j}$ is to use their relative error:

$$\Delta_1(\boldsymbol{\mu}) = \sum_{i=1}^n \sum_{j=1}^k \left(\frac{\omega_{i,j}^F(\boldsymbol{\mu}) - \omega_{i,j}}{\omega_{i,j}} \right)^2 \quad (3)$$

The damage factor $\boldsymbol{\mu}$ that minimizes the objective function $\Delta_1(\boldsymbol{\mu})$ represents the identified structural damage. However, the objective function defined as in eq. (3) turns out in practice to require a very accurate FE model to yield reliable results: the accuracy of damage identification is highly sensitive to the accuracy of the established FE model. When the FE model is not precise, eq.(3) can result in considerable errors. Therefore, a modified objective function is proposed, as shown in eq. (4), where the relative error from eq. (3) is replaced by the MAC value, see eq. (5):

$$\Delta_2(\boldsymbol{\mu}) = \sum_{j=1}^k \left(1 - \text{MAC}(\boldsymbol{\omega}_j^F(\boldsymbol{\mu}), \hat{\boldsymbol{\omega}}_j) \right) + \lambda \|1 - \boldsymbol{\mu}\|_1 \quad (4)$$

$$\text{MAC}(\boldsymbol{\omega}_j^F(\boldsymbol{\mu}), \hat{\boldsymbol{\omega}}_j) = \frac{(\boldsymbol{\omega}_j^F(\boldsymbol{\mu}) \hat{\boldsymbol{\omega}}_j)^2}{\|\boldsymbol{\omega}_j^F(\boldsymbol{\mu})\|^2 \|\hat{\boldsymbol{\omega}}_j\|^2} \quad (5)$$

In eq. (4), the term $\lambda \|1 - \boldsymbol{\mu}\|_1$ represents the l_1 -norm of $1 - \boldsymbol{\mu}$, and including such a term is a typical approach that promotes sparsity of the identified damage³⁷. With eq. (3), a precise FE model is required, so the model of the damaged structure can simulate the actual damaged structure. Replacing the relative frequency residual in eq. (3) with the correlation-based error of the frequency-position relation curves in eq. (4) can decrease the dependence on the accuracy of the FE model because it does not require a precise FE model.

2.3. Mass selection based on local structural sensitivity analysis

An important step in the proposed approach is to select the proper value of the mass to be added. An approach first outlined in Hou et al.¹⁴ is followed here: in order to be conducive to damage identification, added masses should improve structural sensitivity with respect to damage. The sensitivity of the i th natural frequency with respect to the damage factor μ_l , computed for the structure with an additional mass m added at the j th position, can be expressed as

$$R_{ij,l}(\boldsymbol{\mu}, m) = \frac{\partial \omega_{i,j}(\boldsymbol{\mu}, m)}{\partial \mu_l} = \frac{\boldsymbol{\Psi}_{ij}^T(\boldsymbol{\mu}, m) \mathbf{K}_l \boldsymbol{\Psi}_{ij}(\boldsymbol{\mu}, m)}{2\omega_{i,j}(\boldsymbol{\mu}, m)}, \quad (6)$$

where $\boldsymbol{\Psi}_{ij}(\boldsymbol{\mu}, m)$ denotes the respective mode shape vector and \mathbf{K}_l represents the stiffness matrix of the l th substructure, see eq.(2). Based on eq.(6), a sensitivity analysis of the FE model of the original undamaged structure can be performed in order to select the mass that roughly results in the maximum sensitivity of the substructure with respect to damage.

3. MULTI-MODEL DATA FUSION FOR DAMAGE IDENTIFICATION

In practical engineering, obtaining and updating an accurate FE model might be difficult or hardly possible. In such a case, it is proposed here to establish several approximate FE models and use them simultaneously for damage identification purposes. The respective identification results are then integrated using the Dempster-Shafer(D-S) evidence theory to generate a single, accurate result. Such an approach relaxes the requirement for an accurate FE model, and it thus positively contributes to the practical applicability of the method. The D-S evidence theory is one of the fundamental approaches to multi-model data fusion, which can be used to integrate different multi-source information to produce an accurate and complete judgment. The basic concepts of the D-S evidence theory in application to the considered problem are as follows.

Let the damaged and undamaged states of the i th substructure be denoted as $A_{i,d}$ and $A_{i,u}$, respectively. According to the D-S evidence theory, the frame of discernment can be defined as $\Omega_i = \{A_{i,d}, A_{i,u}\}$, and its power set is $2^{\Omega_i} = \{\emptyset, A_{i,d}, A_{i,u}, \Omega_i\}$. The basic probability assignment (BPA), a basic measure in the D-S evidence theory, is a mapping $q: 2^{\Omega} \rightarrow [0,1]$ that satisfies the following properties:

$$\sum_{A \in 2^{\Omega}} q(A) = 1, \quad (7)$$

$$q(\emptyset) = 0. \quad (8)$$

As defined in Section 2.2, μ_j is the ratio of the stiffness of the j th substructure after and before being damaged. Let the corresponding damage extent be defined as $\alpha_j = 1 - \mu_j$. The identified extent $\alpha_j = 0$ indicates that the j th substructure is not damaged, while $\alpha_j = 1$ indicates that it is fully damaged. The damage extent α_j belongs to the interval $[0,1]$, and it can be thus interpreted in terms of the evidence theory as the belief (or evidence) that the j th substructure is damaged.

Assume that v different approximate FE models are established and used for damage identification. Notice that different approximate FE models yield different results, which can be interpreted as different sources of evidence, or different beliefs, and denoted by q_i :

$$q_i(A_{j,d}) = \alpha_{i,j} = 1 - \mu_{i,j}, \quad (9)$$

where $i = 1, 2, \dots, v$ indexes the approximate FE models and $j = 1, 2, \dots, N$ indexes the substructures. The D-S theory provides a rule that allows these different beliefs q_i to be combined together into a single combined belief q . Such a multi-source evidence is fused into a single combined belief as follows:

$$q(A_{j,d}) = \frac{1}{1 - K_j} \prod_{i=1}^v q_i(A_{j,d}) = \frac{1}{1 - K_j} \prod_{i=1}^v (1 - \mu_{i,j}), \quad (10)$$

where K_j quantifies the conflict between the beliefs,

$$K_j = \sum_{\cap A_j = \emptyset} \prod_{i=1}^v q_i(A_j). \quad (11)$$

When the damage extent α_j of all substructures is small, the calculated $q(A_{j,d})$ is extremely small, and the damage of the structure cannot be obviously determined. Therefore, to overcome this limitation, a normalized damage BPA $\bar{q}(A_{j,d})$ is computed, see eq. (12), which can be used for a more straightforward determination of the position and the degree of the damage:

$$\bar{q}(A_{j,d}) = \frac{q(A_{j,d})}{\sum_j q(A_{j,d})}. \quad (12)$$

4. NUMERICAL EXAMPLES

This part illustrates and verifies the proposed method using two numerical simulation examples: a simply supported beam and a five-span bridge model.

4.1. A simply supported beam

4.1.1. The structure.

A steel simply supported beam, as shown in Fig. 2, has the length of 2 m and the cross-section $0.1 \text{ m} \times 0.008 \text{ m}$. The Young modulus is $E = 2.1 \times 10^{11} \text{ Pa}$ and the density is $\rho = 7850 \text{ kg/m}^3$. Poisson's ratio is 0.3. In order to precisely identify the damage positions, the beam is divided into 40 finite elements and 10 substructures, where each substructure consists of 4 elements. The damage is simulated through stiffness reduction, and two damage scenarios are designed as follows:

- 1) Scenario 1: substructure 3 is damaged, and its stiffness is reduced by 30%;
- 2) Scenario 2: substructures 3 and 7 are damaged, and the stiffness is reduced by 30% and 40%, respectively.

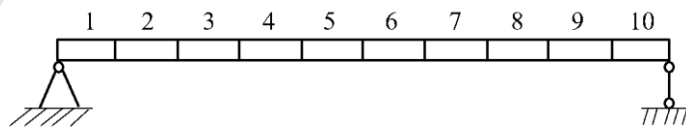


Fig. 2. The simply supported beam and its division into substructures

4.1.2. The influence of the added mass

In order to study the influence of the added mass on the natural frequencies, the mass is initially set to 0.6 kg, 1.2 kg and 2.0 kg and applied in Scenario 1. A pulse excitation is used to simulate an excitation with a modal hammer. The sampling frequency is 10 kHz.

In a practical application, measured data is influenced by the environment and the measurement system, and the measured response has some errors with respect to the real structural response. To verify the effectiveness and robustness of the proposed method, the simulated excitations and responses are numerically contaminated with noise at the level of 5% root mean square (rms), as shown in eq.(13) and eq.(14). If the response is an n -element row vector \mathbf{r} , then the rms of \mathbf{r} is denoted by σ_r and the noise-contaminated vector is calculated as $\mathbf{r}_{\text{noise}}$:

$$\sigma_r = \sqrt{\frac{\|\mathbf{r}\|_2}{n}}, \quad (13)$$

$$\mathbf{r}_{\text{noise}} = \mathbf{r} + 0.05 * \sigma_r * \text{randn}(1,n), \quad (14)$$

where $\text{randn}(1,n)$ is a function that generates an n -element row vector with elements independently drawn from the standard normal distribution. The excitation is contaminated with 5% noise in a similar way.

After the excitation is applied, the simulated acceleration response of the system is recorded as a measured response and used for modal analysis by the Eigensystem Realization Algorithm (ERA)³⁸. Fig. 3 shows the variation of the first four identified natural frequencies with the value of the added mass and its position along the considered beam.

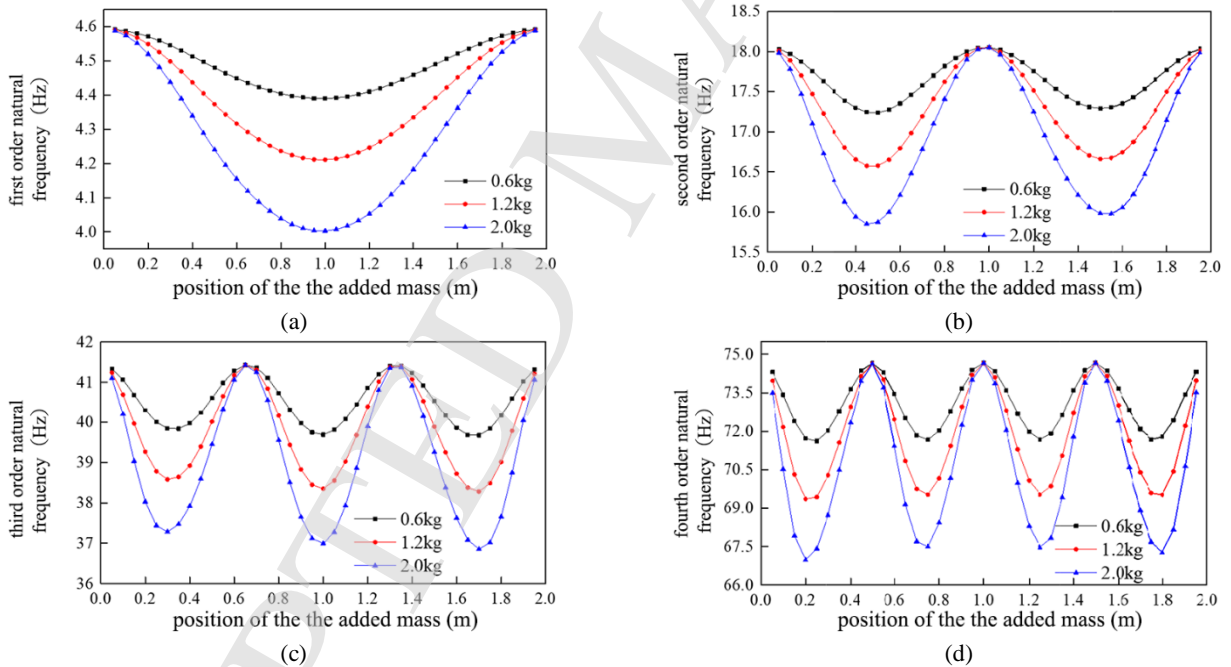


Fig.3. The first four natural frequencies in dependence on the added mass and its position: (a) First order natural frequency, (b) Second order natural frequency, (c) Third order natural frequency, (d) Fourth order natural frequency.

It can be seen in Fig. 3 that a mass added near any of the (supported) ends of the beam has a very little impact on the natural frequency. However, if the mass is added in other positions of the beam, the natural frequencies of the system decrease as the added mass increase. This trend is most obvious in antinodes of the respective mode shapes.

For the purpose of damage identification, a mass should be used that ensures a possibly large discrepancy between the natural frequencies of the damaged structure with the added mass and those of the undamaged structure. Since the damage is not known in advance, based on sensitivity analysis of the undamaged state¹⁴ and Fig. 3, the mass to be used in the numerical experiment is selected as 1.5 kg.

4.1.3. Damage identification

First, the accurate (reference) FE model of the simply supported beam structure without any additional mass is established and analyzed. The theoretical first four natural frequencies of the beam in the undamaged state and in damage Scenarios 1 and 2 are listed in Table 1.

Table1. The first four natural frequencies of the beam without added masses (Hz)

Order of the natural frequency	First	Second	Third	Fourth
Natural frequencies of undamaged structure	4.690	18.762	42.216	75.059
Natural frequencies of damaged structural system in scenario 1	4.592	18.053	41.433	74.660
Natural frequencies of damaged structural system in scenario 2	4.377	17.350	41.200	71.433

As expected, natural frequencies are found to decrease with the increasing degree of structural damage. Based on the change of the frequencies, it can be preliminarily judged that the structure is damaged, but the position of the structural damage and its extent cannot be directly determined. Adding a 1.5 kg mass to the damaged beam in different position allows much more modal information to be obtained. The changes of the natural frequencies with the position of the added mass in different scenarios are depicted in Fig. 4.

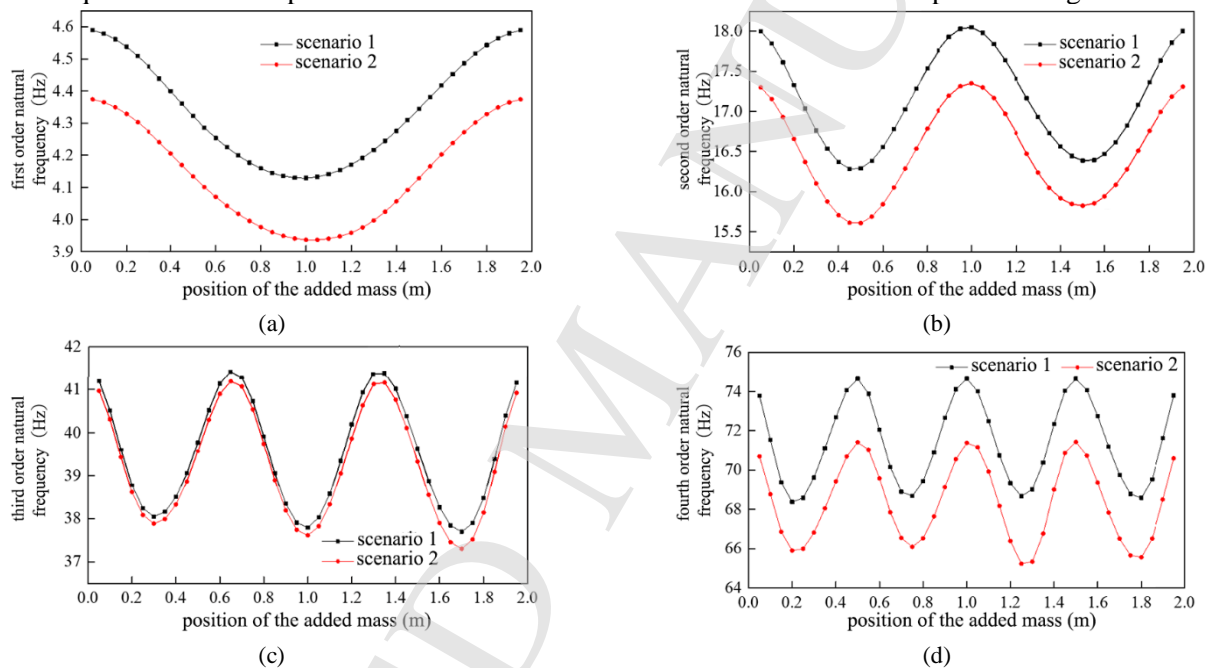


Fig.4. The first four natural frequencies under different damage scenarios in dependence on the position of the added mass: (a) First order natural frequency, (b) Second order natural frequency, (c) Third order natural frequency, (d) Fourth order natural frequency.

It can be seen in Fig. 4 that when the added mass changes its position along the beam, the natural frequencies of the system vary considerably: they have local maxima and minima and the curve is relatively smooth. There are no obvious discontinuity points or other local information that can directly denote the damages, although the frequency curves can be expected to contain the respective information that might be revealed by performing the optimization as described in Section 2.

However, structures monitored in practice are relatively complex, and it is usually difficult to build an accurate FE model. As described in Section 3, it is proposed here to assume that the accurate FE model of the undamaged structure is unknown and to utilize a number of approximate models for the purpose of identification. In this example, the approximate FE models are established by varying the geometric and material parameters such as the width, height and Young's modulus of the structure, see Table 2. These approximate models are then considered as intact models to identify the structural damages.

Table 2. Parameters of the considered approximate structural models

Approximate model No.	width/m	height/m	Young's modulus/GPa
Model 1	0.09	0.008	210
Model 2	0.10	0.009	210
Model 3	0.10	0.008	200

By successively adding the same 1.5 kg mass to each of the three considered FE models, the curves are obtained that relate the first four natural frequencies to the position along the beam, see Fig. 5. The differences between the approximate models affects the frequencies, but the general trends in all the curves remain similar.

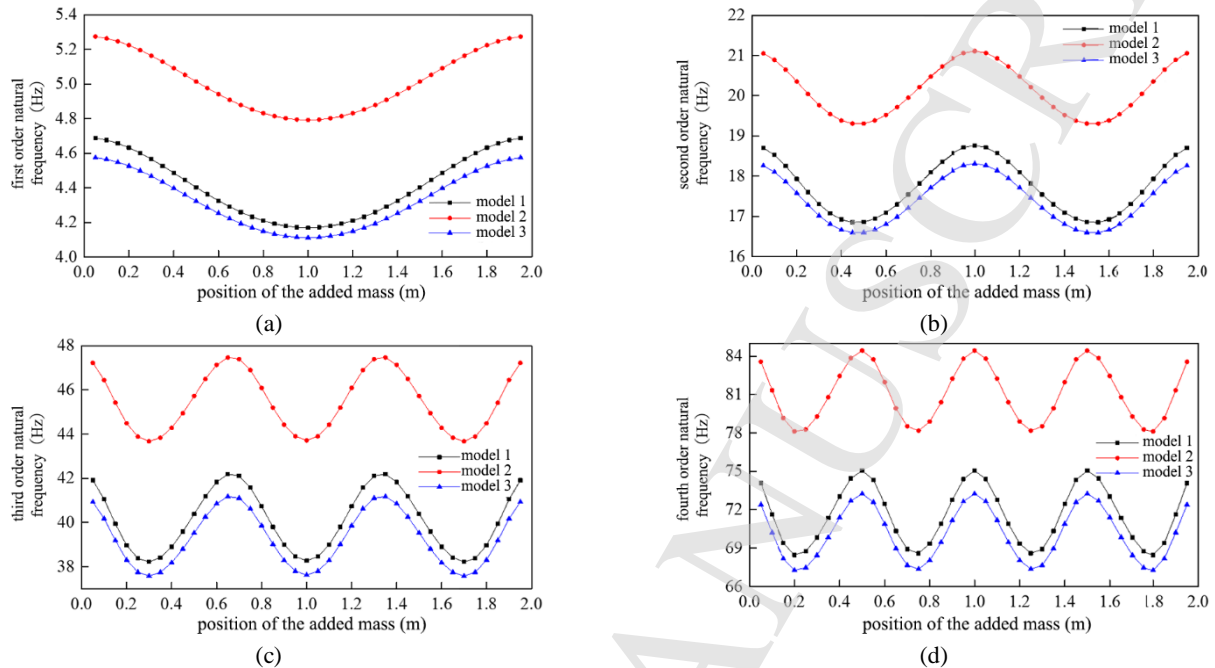


Fig.5. The first four natural frequencies for different approximate models in dependence on the position of the added mass: (a) First order natural frequency, (b) Second order natural frequency, (c) Third order natural frequency, (d) Fourth order natural frequency

Each approximate FE model is successively used to form the objective function eq. (4) and to identify the damage. The results obtained by each model are used as various data sources for data fusion, as described in Section 3. The damage extents identified for each substructure are interpreted as the BPA of each evidence source, and the D-S evidence theory is used to fuse the identification results into a single combined evidence, which then serves to locate and quantify the damage. The obtained results are shown in Fig. 6 and Fig. 7.

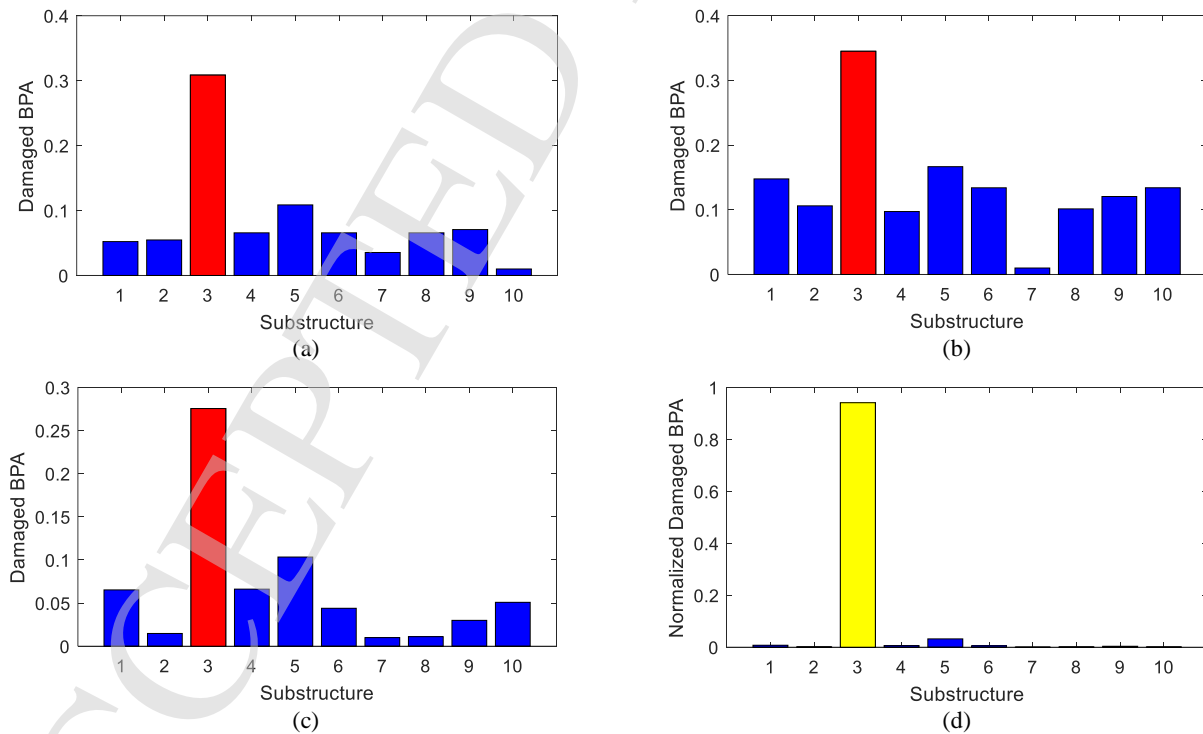


Fig. 6. The identification results for the approximate models and the evidence fusion results for damage Scenario 1: (a) The damage identification result for model 1, (b) The damage identification result for model 2, (c) The damage identification result for model 3,

(d) The damage identification result after fusion of the evidence.

Table 3 lists the BPAs for the damage scenario 1(Fig. 6) and the combined beliefs according to the D-S evidence theory, see eq.(10) to eq.(12). For example, for substructure 1 the approximate models yield $q_1 = 0.108$, $q_2 = 0.166$, $q_3 = 0.103$, so that the belief conflict $K_5 = 0.33085$ is quantified as defined in eq.(11):

$$K_5 = (1 - q_1)q_2q_3 + q_1(1 - q_2)q_3 + q_1q_2(1 - q_3) + (1 - q_1)(1 - q_2)q_3 + (1 - q_1)q_2(1 - q_3)q_3 + q_1(1 - q_2)(1 - q_3). \quad (15)$$

The D-S theory focuses on the common evidence and thus the BPAs for substructure 5 are combined as follows:

$$q(A_{5,d}) = \frac{q_1q_2q_3}{1 - K_5} \approx 0.0028, \quad (16)$$

which after normalization yields the value of 0.0316 listed in Table 3.

Table 3 Basic probability assignments and the combined values for the damage scenario 1

substructure	1	2	3	4	5	6	7	8	9	10
model 1 q_1	0.051	0.054	0.310	0.065	0.108	0.065	0.034	0.065	0.070	0.009
model 2 q_2	0.148	0.105	0.345	0.097	0.166	0.134	0.008	0.100	0.121	0.134
model 3 q_3	0.065	0.0138	0.275	0.066	0.103	0.044	0.009	0.010	0.030	0.050
$q(A_{j,d})$	0.0006	0.0001	0.0824	0.0005	0.0028	0.0005	0.0000	0.0001	0.0003	0.0001
$\bar{q}(A_{j,d})$	0.0074	0.0011	0.9428	0.0060	0.0316	0.0057	0.0000	0.0009	0.0037	0.0008

According to Fig. 6(ac), the information obtained from models 1 and 3 for damage scenario 1 can preliminarily reveal that substructure 3 is damaged, but it is more difficult to directly determine the damage position by analyzing the results of model 2. The identified damage extents are relatively large also for the undamaged substructures. Due to the influence of noise and model inaccuracy, the result from any single model can be treated only as a piece of evidence that is indicative of the actual damage but inaccurate to a significant degree. However, in the process of evidence fusion, the full use of the information available from each model is made. The combined result is found to accurately determine the damage position (substructure 3 in this example) without any significant errors. By fusing the available evidence, more reliable results can be obtained than by using any single information source.

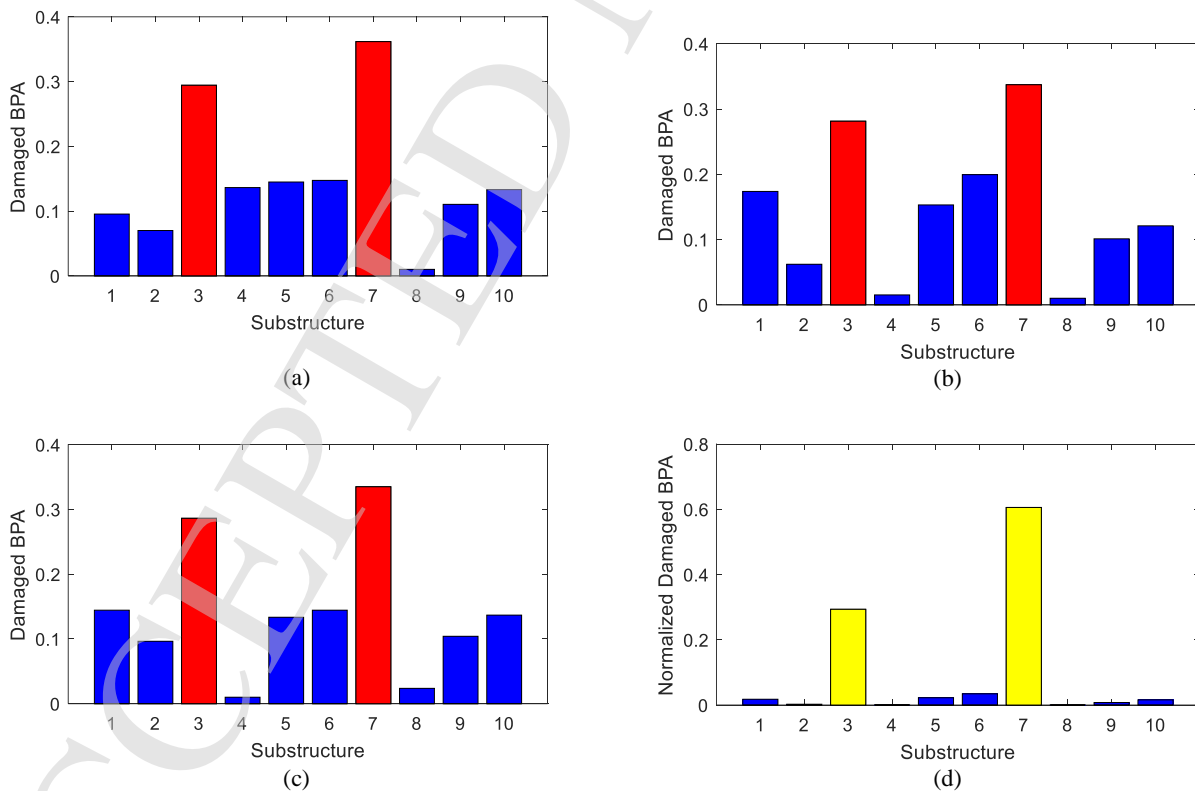


Fig.7. The identification results for the approximate models and the evidence fusion results for damage Scenario 2: (a) The damage identification result for model 1, (b) The damage identification result for model 2, (c) The damage identification result for model 3,

(d) The damage identification result after fusion of the evidence.

According to Fig. 7(ac), the results from models 1 and 3 suggest that the substructures suspected of damage are 3 and 7. According to the results of model 2, one can suspect substructures 3, 6 and 7. Especially for model 2, the damage extents identified for other substructures are relatively high and might suggest a wide-area damage of low intensity. If the structure is damaged in more than one position, a misjudgment can easily occur, if a single inaccurate model is used for identification. As in the previous example, the combined result obtained by fusing the evidence available from all three models is much more accurate than any single-source result and can be used to directly locate the damages of the substructures (substructures 3 and 7 in this example).

4.2. A large span bridge

4.2.1. Overview of the bridge

The following paragraphs employ a model of a large span box section bridge for damage identification. The main span is made of prestressed concrete and it is a nonflexible frame-continuous integrated beam. The length of the bridge main span is $116.4\text{ m} + 200\text{ m} + 220\text{ m} + 200\text{ m} + 116.4\text{ m} = 852.8\text{ m}$, as shown in Fig. 8. The bridge is a box section bridge, and in order to reduce its mass, it is designed with one single box and one single chamber. Its top width is 12.8 m and the bottom width is 6.0 m, while the top plate thickness is 0.28 m. The cantilever length is 3.4 m, and the thickness of the cantilever root is 0.75 m. The main pier has a double thin-wall rectangular section made of reinforced concrete with the wall thickness of 1.8 m and the center distance of 8 m. Other bridge sections are rectangular and also made of reinforced concrete. The foundation of the bridge is drilling perfusion piles.

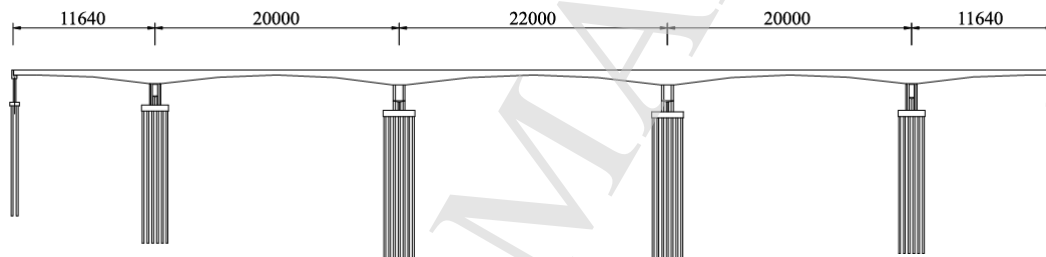


Fig. 8. Overview of the considered bridge

4.2.2. The FE model

The finite element BEAM188 of ANSYS is used to build the FE model of the bridge, ignoring the prestressed tendons in the structure. The bridge model is shown in Fig. 9. The bottom sections of the piers are fixed, while the horizontal and vertical DOFs of the top of the piers and the bottom of the box girders are coupled. The tops of the rigid frame piers (Fig. 10a) are fixed with the bottom sections of the beam. In addition, COMBIN14 element is used to simulate the influence of the expansion joints at the end of the box beam.

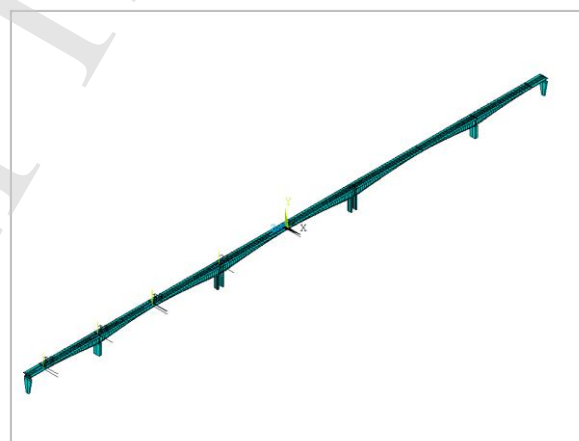


Fig. 9. The FE model of the bridge

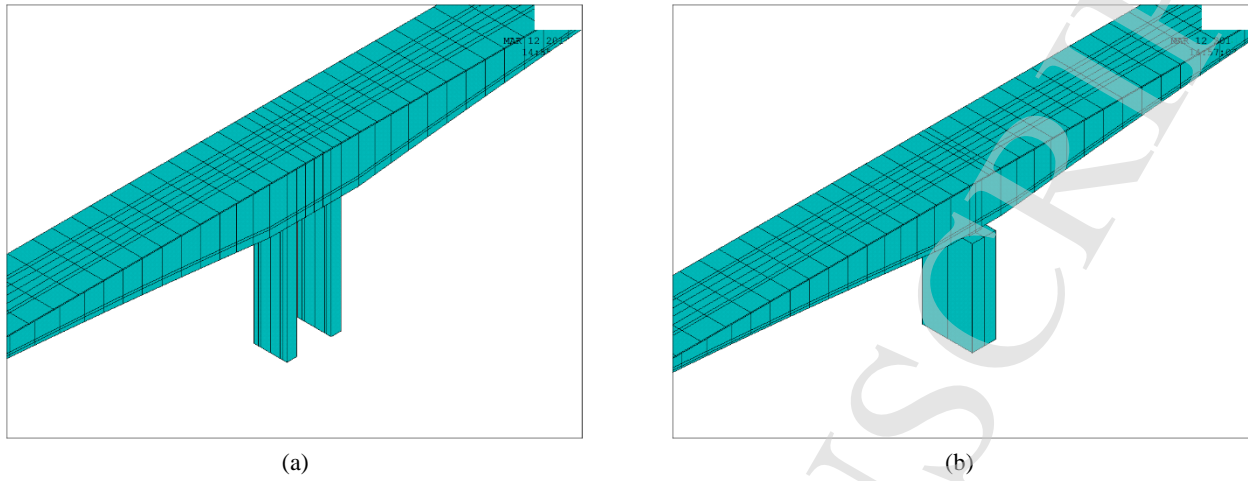


Fig. 10. Models of the bridge piers: (a) Rigid pier, (b) Non-rigid pier

4.2.3. Model reduction and approximate FE models

The FE model of the bridge is built in the ANSYS environment. The structural stiffness and mass matrices are then exported from ANSYS and imported into MATLAB for further processing and to simulate the process of structural damage identification. To improve the efficiency of numerical analysis, the Guyan model reduction is used in MATLAB to reduce the number of bridge DOFs. As the most important displacements occur in the vertical direction (Z-direction), the reduction preserves the vertical DOFs of the original detailed model and reduces all the remaining DOFs. After model reduction, the total number of the DOFs is sharply reduced to only 113 vertical DOFs, which not only improves the numerical effectiveness of the analysis but also facilitates the optimization of the structure.

The first eight natural frequencies of the detailed model and the reduced model are listed for comparison in Table 4. The corresponding eight mode shapes for both models are shown and compared in Fig. 11. The natural frequencies and the mode shapes of both models are almost identical, which confirms that the reduced model preserves the important dynamic characteristics of the original detailed model. The reduced model and its natural frequencies are thus used for damage identification.

Table 4. Natural frequencies before and after model reduction (Hz)

The order of the natural frequency	1	2	3	4	5	6	7	8
Original detailed model (vertical)	0.6973	0.7464	0.9628	1.4193	1.5084	1.9897	2.4138	2.6019
Reduced model	0.6970	0.7459	0.9627	1.4192	1.5083	1.9900	2.4140	2.6021

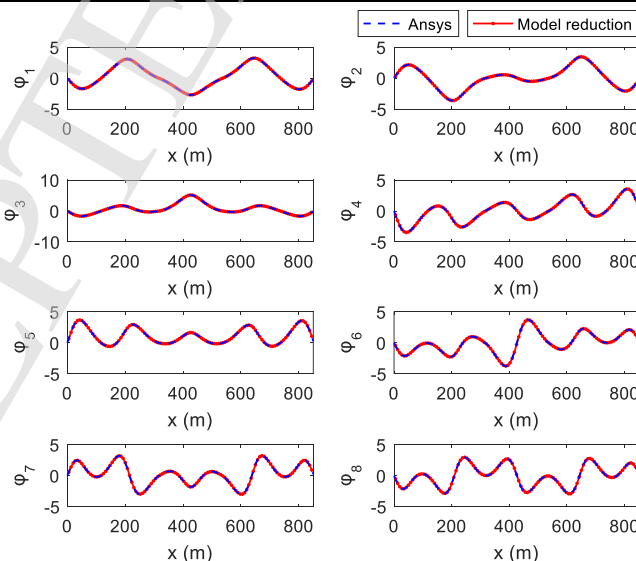


Fig. 11. The first eight modal shapes of the bridge: original detailed model (ANSYS) and after model reduction

As the approximate FE models used for the purpose of damage identification, five different models are provided based on the reduced model described above. Model inaccuracies were simulated by modification of material Young's modulus and density (structural stiffness and/or mass), as listed in Table 5.

Table 5. The parameters of the approximate FE models

Approximate model	Stiffness modification ratio	Density modification ratio
Model 1	1.10	1.0
Model 2	0.90	1.0
Model 3	1.00	0.9
Model 4	0.95	0.9
Model 5	0.80	0.9

4.2.4. Damage identification

The entire deck of the bridge is treated as a subject to identification. It is divided into 15 substructures as shown in Fig. 12. The stiffness of substructure 4 and substructure 8 are reduced by 50% at the same time. In the entire process, 5% white noise is considered for measurements.

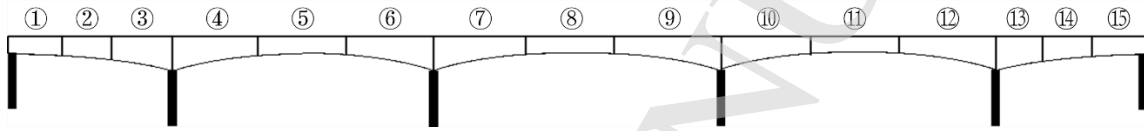


Fig. 12. Division of the bridge deck into 15 substructures

The additional mass is successively added to the bridge at different positions along the deck. Similarly as in Section 4.1, by analyzing the effects of different masses, the value of the added mass is determined to be 500 tons. The first eight natural frequencies of the bridge before and after damage are used in the identification process, and the first two of them are shown in Fig. 13. The frequencies of the damaged structure are slightly lower, and their spatial variation can be expected to contain the information about the damage.

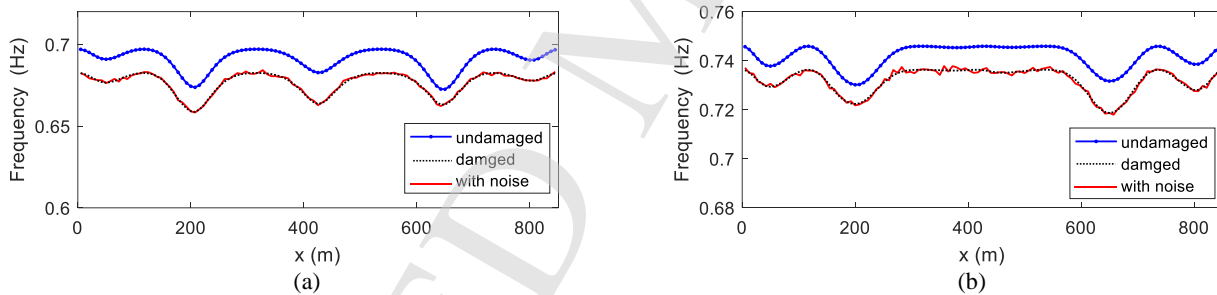
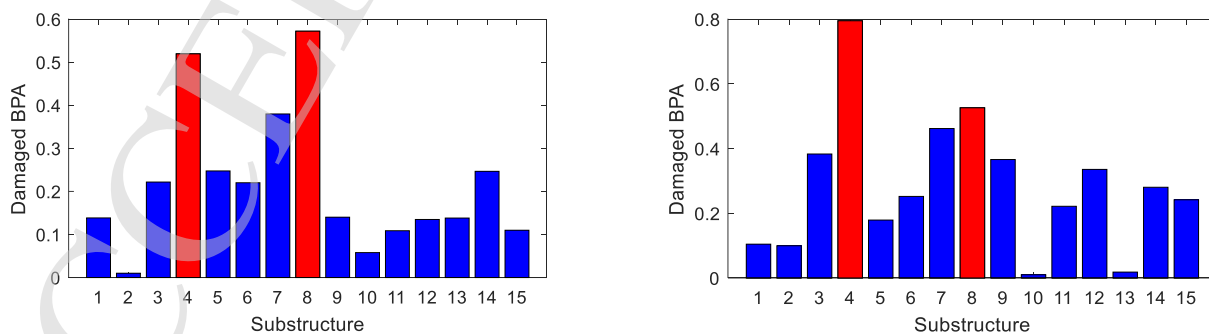


Fig. 13. The first two natural frequencies of structure in dependence on the position of the added mass: (a) First natural frequency of the bridge, (b) Second natural frequency of the bridge.

The identification is performed by updating all five approximate FE models listed in Table 5 and optimizing the MAC-based objective function, as defined in eq. (4) and computed for the first eight natural frequencies (with noise). The five obtained results are shown in Fig. 14(a)~(e). The D-S data fusion method is then used to combine the evidence. Fig. 14(f) shows the results obtained by fusing the results from models 1, 2 and 4. Fig. 14(g) shows the results obtained by fusing the results from models 1, 4 and 5. Finally, all five available results are fused, and the combined result of models 1~5 is shown in Fig. 14(h).



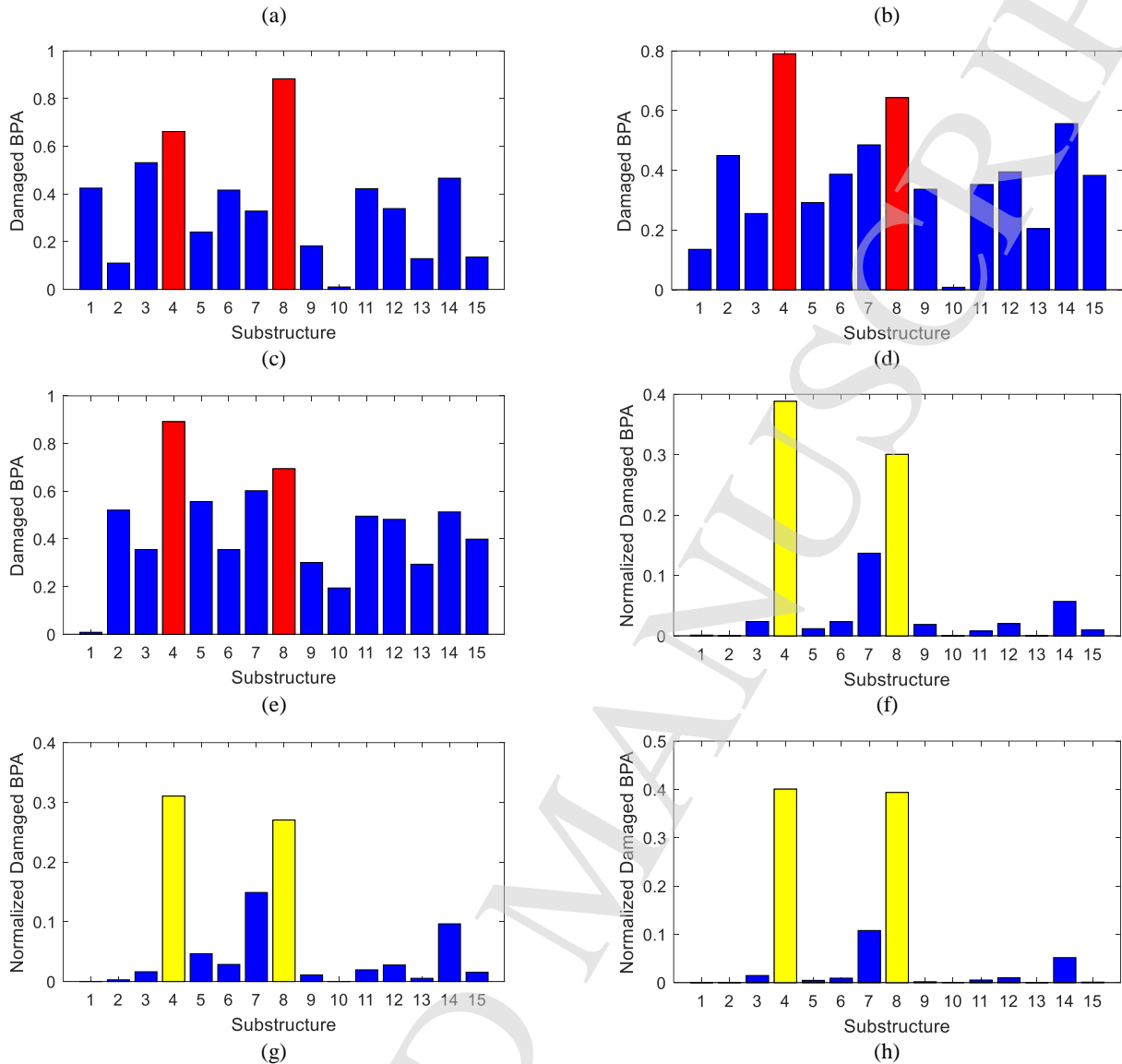


Fig. 14. Damage identification result for single approximate models and after data fusion: (a) using model 1, (b) using model 2, (c) using model 3, (d) using model 4, (e) using model 5, (f) data fusion using models 1, 2 and 4, (g) data fusion using models 1, 4 and 5, (h) data fusion using models 1~5

It can be seen from Fig. 14 that if only models 1, 2 and 4 are used for data fusion, the actually damaged substructures 4 and 8 are properly identified, but substructure 7 can be also suspected of being damaged. Similarly, if only models 1, 4 and 5 are used for data fusion, substructures 7 and 14 can be suspected of being damaged. However, if all the available evidence is combined (models 1~5), substructures 4 and 8 stand out much more clearly as the only substructures being damaged. Overall, the proposed method can accurately identify positions of the damage and is highly accurate also in applications to large structures such as bridges.

5. EXPERIMENTAL STUDY

5.1. Instrumentation

The experimental devices include a modal hammer (Fig. 15a), an acceleration sensor (Fig. 15b), and a signal acquisition unit (Fig. 15c). The modal hammer is used to exert a pulse excitation to the structure. During the experiment, the excitation could be recorded by the internal force sensor of the hammer. The acceleration sensor is a single axis accelerometer (model number 333B50 SN LW52869). The signal acquisition unit used in the experiment is NI USB-4431 from National Instruments (NI).

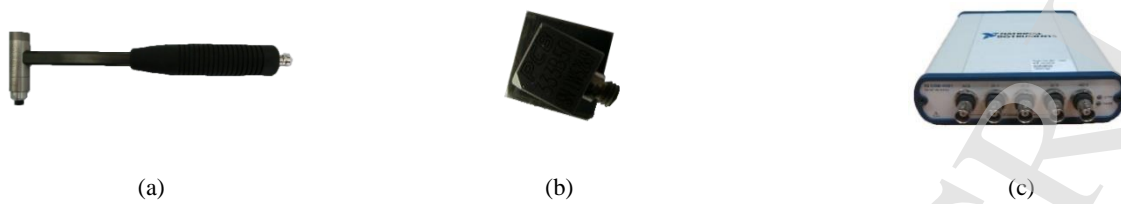


Fig. 15. Experimental devices: (a) Modal hammer, (b) Acceleration sensor, (c) Signal acquisition unit

5.2. Cantilever beam and the experimental process

A laboratory steel cantilever beam is used in this experiment, see Fig. 16. The length is 0.84 m, while the cross-section has the dimensions of $0.078 \text{ m} \times 0.0068 \text{ m}$. The total mass is 3.5 kg. The beam is fixed by two steel plates with a thickness of 1 cm and bolts joining the steel plate and the foundation. The foundation is a steel structure with a large weight and stiffness, which satisfies the experimental requirements. The additional mass of 0.3 kg is designed and attached during the experiment at different positions of the beam by a strong magnet. Two such beams are physically fabricated: the first one is the original intact structure and the second one is the damaged beam. The damage is introduced in the form of a series of symmetrical slits that cover 14 cm length of the beam and simulate its local reduction of stiffness, see Fig. 16. Each slit is through-thickness, 15 mm in depth and 1 mm in width, and it is cut pairwise, symmetrically on both sides of the beam.

The damaged cantilever beam is divided into 12 sections, and 1 acceleration sensor is arranged on the lower side of the middle of the beam (Fig. 16). Then the additional mass of 0.3 kg is successively attached at 11 positions of the upper side of the beam (in the right end of sections 1 to 11) by a magnet. For the additional mass fixed in each of these positions, the impact excitation is applied and the corresponding acceleration signals from the accelerometer are collected; such a procedure is repeated 10 times. Thus, a total of 110 acceleration signals (11 mass positions \times 1 accelerometer \times 10 impact excitations) are collected. A typical excitation and a typical acceleration response are shown in Fig. 17. The collected signals are imported into MATLAB for further processing and damage identification. In particular, the acceleration responses are analyzed by the ERA method³⁸ to identify the natural frequencies of the damaged structure without the mass and with the mass added at different sections of the beam.

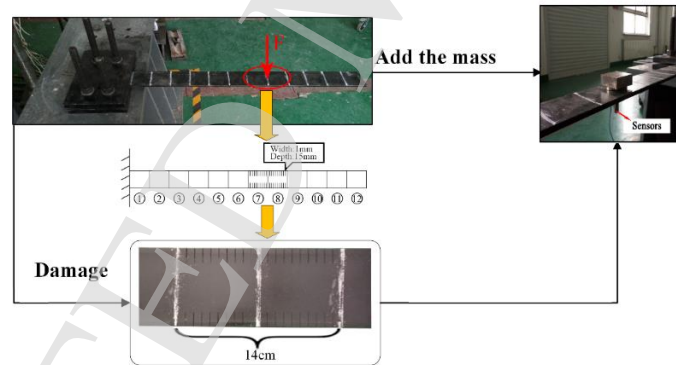


Fig. 16. Cantilever beam, the damage and the fixed concentrated mass

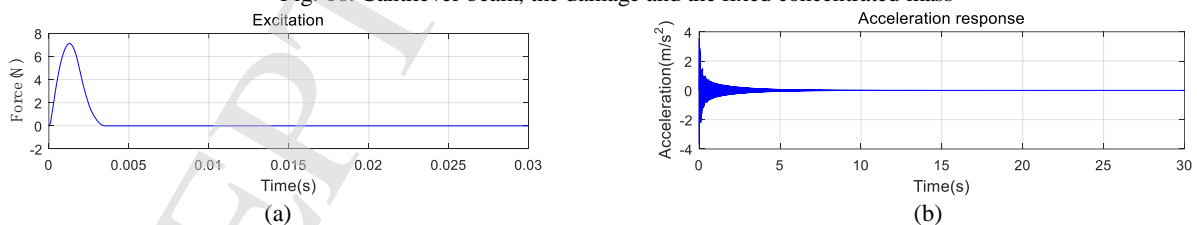


Fig. 17. Typical impact hammer excitation and an acceleration response:(a) Excitation, (b) Acceleration response

5.3. FE model of the cantilever beam and modal analysis

An initial FE model of the undamaged cantilever beam is built based on the geometrical dimensions of the experimental specimen, as stated in Section 5.2, and the catalogue material parameters of the employed steel: Young's modulus of 237 GPa and the density of 7850 kg/m^3 . The first four natural frequencies of the model are listed in Table 6 and compared to the experimentally determined natural frequencies of the undamaged

physical beam. The relative errors of the first four natural frequencies between the FE model and the experimental beam are less than 2%, which satisfies the engineering request and indicates that the established FE model has an adequate accuracy.

Table 6. The first four natural frequencies of the physical undamaged beam and its FE model

The order of the structural natural frequency	1st order	2nd order	3rd order	4th order
FE model (Hz)	8.05	50.46	141.29	276.88
Experimental model (Hz)	8.15	51.22	143.18	281.46
Error	1.2%	1.5%	1.3%	1.6%

The additional mass of 0.3 kg is added from left to right to the damaged experimental beam to perform the measurements as described in Section 5.2. At each position, the first four natural frequencies are determined and compared to the theoretical, model-based frequencies, which is shown in Fig. 18.

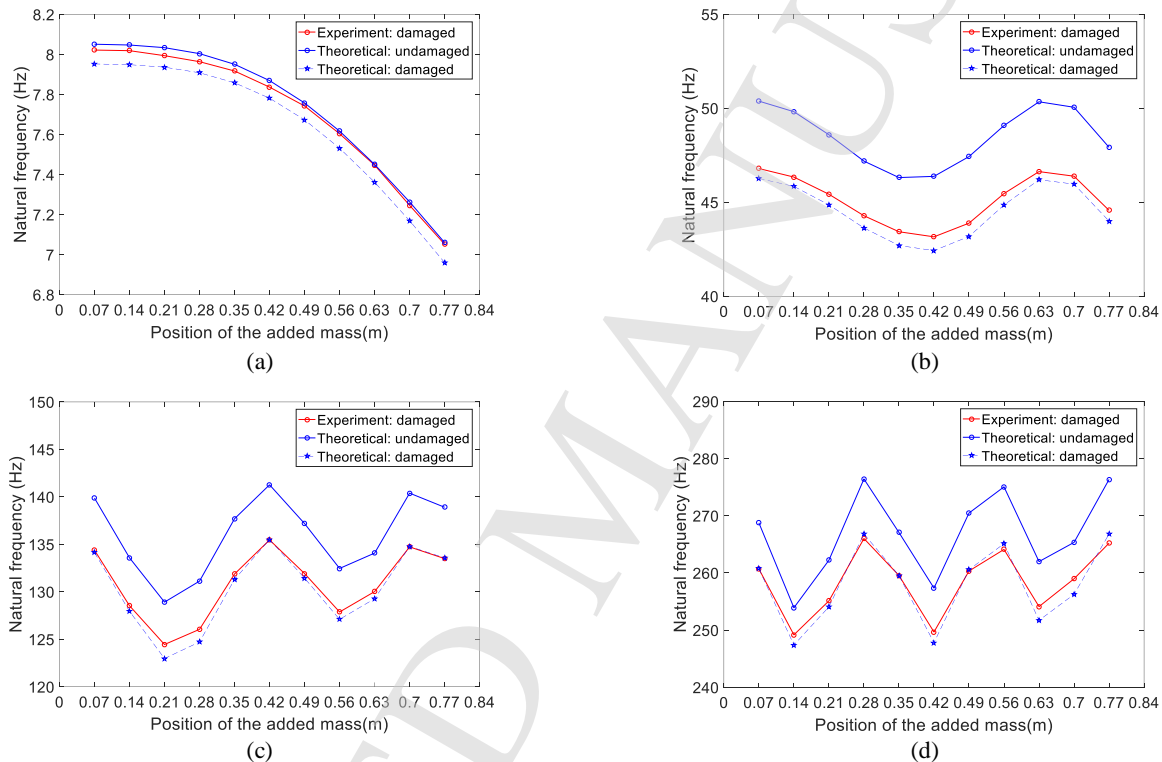


Fig. 18. The theoretical and experimental first four natural frequencies of the structure: (a) The first order natural frequency, (b) The second order natural frequency, (c) The third order natural frequency, (d) The fourth order natural frequency

The frequencies obtained experimentally slightly differ from the theoretical frequencies obtained using the FE model of the damaged beam. As in Table 6, the relative differences are less than 2% and can be attributed to small inaccuracies of the FE model. Due to damage, the experimental frequencies (damaged beam) generally decrease with respect to the theoretical frequencies of the undamaged beam, which indicates that the structure is damaged. However, the frequency curves of the experimental beam are relatively smooth without any obvious discontinuities, so that they cannot be used for any direct determination of the damage position.

5.4. Approximate FE models

The geometric and material parameters of the physical beam used in the experiment might not be accurately known for a number of reasons: the steel might not be accurately cut during the manufacturing process, there might be errors when measuring its dimensions, the elastic modulus of the steel might not be accurately known, etc. Therefore, the established FE model might not exactly match the experimental cantilever beam. As proposed in this paper, three similar approximate FE models are established by varying the width, height and Young's modulus, see Table 7. These three models are then concurrently used in the process of damage

identification.

Table 7. Parameters of the physical cantilever beam and of its three approximate FE models

	Physical	FE model 1	FE model2	FE model3
width/mm	78	80	78	80
height/mm	6.8	6.8	8.0	8.0
Young's modulus/GPa	237	237	237	225

5.5. Damage identification

Two damage scenarios are designed and tested: a single damage scenario and a scenario with two damages.

5.5.1. Single damage

The slit (mentioned in Section 5.2 and shown in Fig. 16) is regarded as a single damage. That is, the cantilever beam is divided into 6 substructures, each comprised of two sections that are assumed to share the same stiffness reduction ratio (the damage parameter to be identified). The position of the actual damage is the 4th substructure. The identification results are shown in Fig. 19.

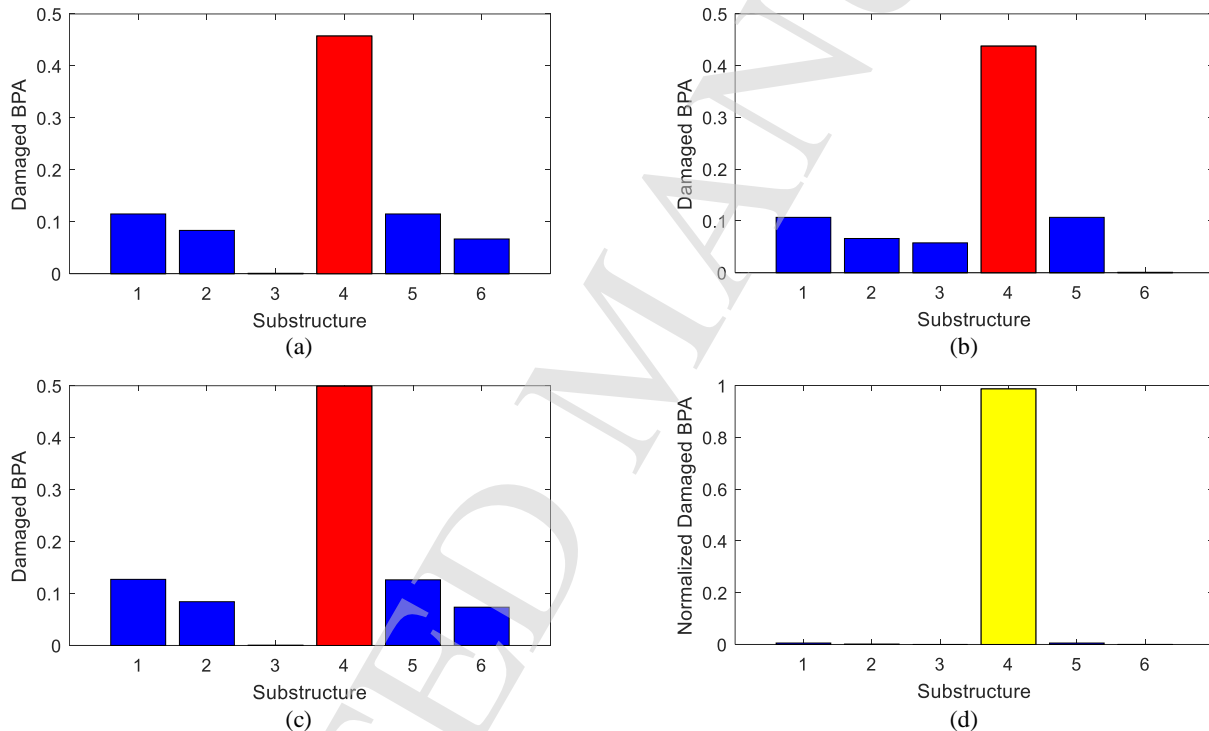


Fig. 19. The identification results for a single damage: (a) Identification for the approximate model 1, (b) Identification for the approximate model 2, (c) Identification for the approximate model 3, (d) Combined result after data fusion

It can be seen from Fig. 19 that all three models can be independently used for an initial determination that substructure 4 is damaged, despite the varying length, height and Young's modulus. However, if the evidence available from the three models is combined by data fusion, the result is more accurate with a much more unambiguous identification of the damage position. Even in the simple case of a single damage, data fusion helps to avoid misjudgment.

5.5.2. Multiple damages

The slit (mentioned in Section 5.2 and shown in Fig. 16) is regarded as two separate damages. That is, the cantilever beam is divided into 12 substructures for a higher resolution, and the damage position is the 7th and 8th substructure. The identification results are shown in Fig. 20.

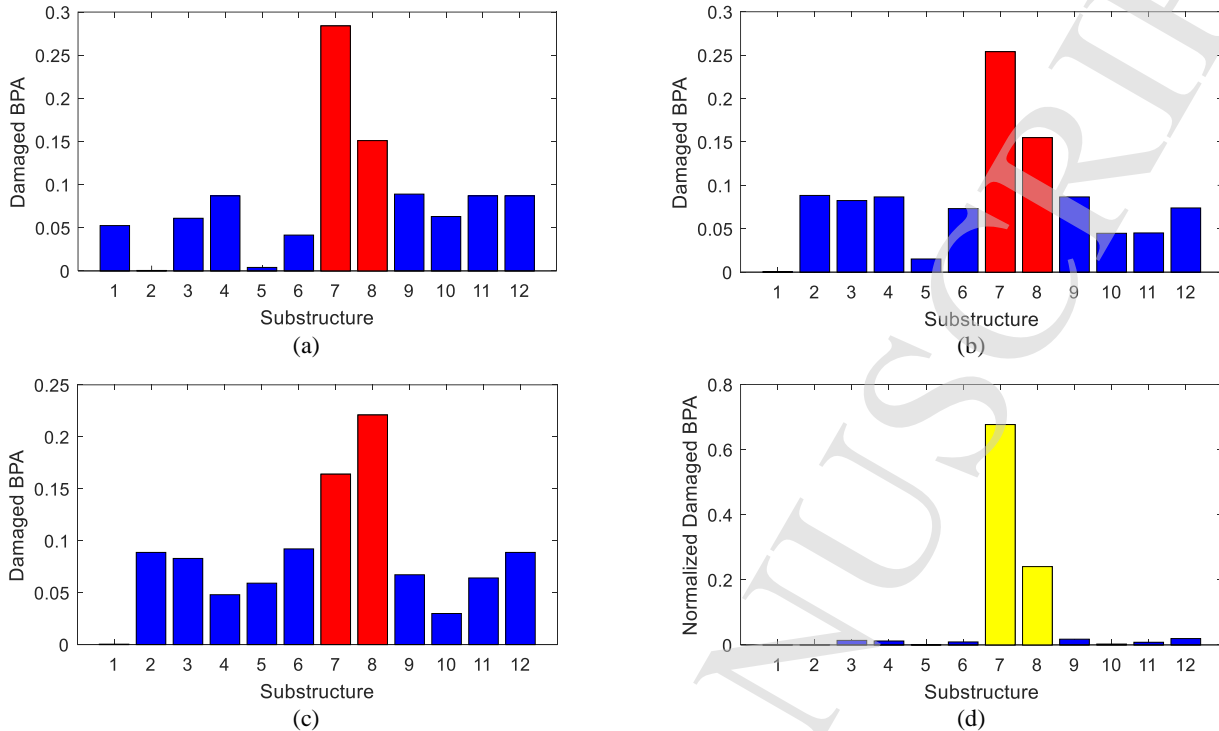


Fig. 20. The identification results for multiple damages: (a) Identification for the approximate model 1, (b) Identification for the approximate model 2, (c) Identification for the approximate model 3, (d) Combined result after data fusion

According to the identification result obtained based on model 1, it can be preliminarily determined that the damage position is substructure 7, while substructure 8 might be suspected of being damaged. Model 2 can preliminarily determine that substructures 7 and 8 are damaged, but at the same time other substructures may be misjudged, because their identified damage extents are also relatively large. Similarly, the identification results of model 3 show that substructures 7, 8 are probably damaged, but damages of other substructures cannot be excluded. However, the combined results obtained with the evidence theory by fusing the results available from the three approximate models can directly and unambiguously determine that substructures 7 and 8 are damaged, while the other substructures are almost certainly intact. The identification result obtained by multi-source data fusion describes the physical structure better than any of the partial approximate models: the result is more accurate and credible.

Throughout the above analysis, it can be recognized that, theoretically, the more approximate models are used, the better the data fusion results are. However, using more models means also more time is consumed for model building and optimization of parameters. The gathered experience suggests that 3-5 approximate models might be recommended to perform data fusion, in order to balance the accuracy and efficiency of damage identification.

6. CONCLUSION

This paper aims to address the three following problems that often hinder practical implementations of SHM systems: (1) Modal data available in practice is scarce and insensitive to local damages. (2) Identification results are sensitive to noise. (3) Identification process relies heavily on the accuracy of the employed FE model of the structure. The approach described here proposes and combines two methods:

1. *Mass addition.* Modal data is repeatedly collected for the damaged structure with an additional pointwise mass added in various positions. Such a locally added mass increases the amount of modal data and its sensitivity to local damages. A MAC-based objective function is then proposed to evaluate the collected modal data as an ensemble.
2. *Data fusion.* The sensitivity to noise and the dependence on a precise FE model are relaxed by performing repeated identifications based on approximate FE models of the monitored structure. Each of the approximate results obtained this way, when considered separately, is much less accurate than the result potentially obtained using a highly accurate FE model and noise-free data. However, the

approximate results are then interpreted as the available pieces of evidence in the framework of the Dempster-Shafer evidence theory. The corresponding data fusion process is performed to combine them into a single, accurate and reliable result.

The proposed approach, by increasing the amount and sensitivity of modal information and by fusing multiple approximate FE models, can be used for accurate identification of structural damages. The effectiveness of the method is verified by numerical simulation of a simply supported beam and a long-span bridge, as well as in an experiment of a physical cantilever beam.

Disclosure statement

No potential conflict of interest was reported by the authors.

Acknowledgment

The authors gratefully acknowledge the support of National Key Research and Development Program of China (Grant No.2018YFC0705604), of the National Natural Science Foundation of China (NSFC) (Grant No.51878118), of Liaoning Provincial Natural Science Foundation of China (Grant No.20180551205), of the Fundamental Research Funds for the Central Universities (Grant No.DUT19LK11), and of the National Science Centre, Poland (Grant No.2018/31/B/ST8/03152).

References

1. C.Tsogka, E. Daskalakis, G. Comanducci and F. Ubertini, The stretching method for vibration-based structural health monitoring of civil structures, *Computer-Aided Civil and Infrastructure Engineering*, **32**(4)(2017) 288-303 doi:10.1111/mice.12255
2. D. Giagopoulos, A. Arailopoulos, V. Dertimanis, C. Papadimitriou, E. Chatzi and K. Grompanopoulos, Structural health monitoring and fatigue damage estimation using vibration measurements and finite element model updating, *Structural Health Monitoring* **18**(4)(2018) 1-18 doi:10.1177/1475921718790188
3. Q. Huan, M. Chen, Z. Su and F. Li, A high-resolution structural health monitoring system based on SH wave piezoelectric transducers phased array, *Ultrasonics* **97**(2019) 29-37 doi:10.1016/j.ultras.2019.04.005
4. M. Jahangiri, M. A. Najafgholipour, S.M. Dehghan and M. A. Hadianfard, The efficiency of a novel identification method for structural damage assessment using the first vibration mode data, *Journal of Sound and Vibration* **458**(2019) 1-16 doi:10.1016/j.jsv.2019.06.011
5. Y. B. Yang and J. P. Yang, State-of-the-art review on modal identification and damage detection of bridges by moving test vehicles, *International Journal of Structural Stability and Dynamics* **18**(2) (2018) 1850025 doi:10.1142/S0219455418500256
6. J. He, X. Zhang and B. Xu, Identification of structural parameters and unknown inputs based on revised observation equation: Approach and validation, *International Journal of Structural Stability and Dynamics* **19**(12) (2019) 1950156. doi:10.1142/S0219455419501566
7. M. L. Wang, G. Heo and D. Satpathi, A health monitoring system for large structural systems, *Smart Materials and Structures* **7**(5)(1998)606-616 doi:10.1088/0964-1726/7/5/005
8. M. Maalej, A. Karasaridis, S. Pantazopoulou and D. Hatzinakos, Structural health monitoring of smart structures, *Smart Materials and Structures* **11**(4)(2002) 581 doi:10.1088/0964-1726/11/4/314
9. N.G. Nalitolela, J.E.T Penny and M.I. Friswell, A mass or stiffness addition technique for structural parameter updating, *International Journal of Analytical and Experimental Modal Analysis* **7**(3)(1992) 157-168
10. G.R. Gillich, Z.I. Praisach, M.A. Wahab, N. Gillich, I. C. Mituletu and C. Nitescu, Free vibration of a perfectly clamped-free beam with stepwise eccentric distributed masses. *Shock and Vibration* **2016**(2016)2086274 doi:10.1155/2016/2086274
11. C. Deng, S. Hu and P. Gu, Modal identification and finite element model updating by adding known masses, *Applied Mechanics and Materials* **405-408**(2013) 808-815 doi:10.4028/www.scientific.net/amm.405-408.808
12. E. Lee and H. Eun, Damage identification of a frame structure model based on the response variation depending on additional mass, *Engineering with Computers* **31**(4)(2014) 737-747 doi:10.1007/s00366-

- 014-0384-8
13. W. Zhou, Q. Yang and W. Zhao, Structural damage identification with generalized flexibility and added masses, *Journal of Mechanical Strength***38**(2016) 156-159 doi:10.16579/j.issn.1001.9669.2016.01.029
 14. J. Hou, Ł. Jankowski and J. Ou, Structural damage identification by adding virtual masses, *Structural and Multidisciplinary Optimization***48**(1)(2013) 59–72 doi:10.1007/s00158-012-0879-0
 15. M. Cao and P. Qiao, Integrated wavelet transform and its application to vibration mode shapes for the damage detection of beam-type structures, *Smart Materials and Structures***17**(5)(2008) 055014 doi:10.1088/0964-1726/17/5/055014
 16. M. Wang, H. Lu and P. Deng, Research on structural damage identification of truss structure based on EMD and neural network, *Earth and Environmental Science***267**(2019) 032040 doi:10.1088/1755-1315/267/3/032040
 17. K. Dragomiretskiy and D. Zosso, Variational Mode Decomposition, *IEEE Transactions on Signal Processing***62**(3)(2014) 531–544 doi:10.1109/tsp.2013.2288675
 18. G.R. Gillich and Z.I. Praisach. Modal identification and damage detection in beam-like structures using the power spectrum and time–frequency analysis, *Signal Processing***96**(2014) 29–44. doi:10.1016/j.sigpro.2013.04.027
 19. D. P. Patil and S. K. Maiti, Experimental verification of a method of detection of multiple cracks in beams based on frequency measurements, *Journal of Sound and Vibration***281**(1-2)(2005) 439–451 doi:10.1016/j.jsv.2004.03.035
 20. M. Cao, L. Ye, L. Zhou, Z. Su and R. Bai, Sensitivity of fundamental mode shape and static deflection for damage identification in cantilever beams, *Mechanical Systems and Signal Processing***25**(2)(2011) 630–643 doi:10.1016/j.ymsp.2010.06.011
 21. Z.D. Xu, S.Li and X. Zeng. (2018). Distributed Strain Damage Identification Technique for Long-Span Bridges Under Ambient Excitation. *International Journal of Structural Stability and Dynamics***18**(11) (2018), 1850133. doi:10.1142/s021945541850133x
 22. W. M. West, Illustration of the use of modal assurance criterion to detect structural changes in an Orbiter test specimen, Proceedings of the Air Force Conference on Aircraft Structural Integrity, *NASA Johnson Space Center* (1986) <https://ntrs.nasa.gov/search.jsp?R=19870041253>
 23. L. Deng and C. S. Cai, Bridge model updating using response surface method and genetic algorithm, *Journal of Bridge Engineering***15**(5)(2010) 553–564 doi:10.1061/(asce)be.1943-5592.0000092
 24. B. Jaishi and W. X. Ren, Damage detection by finite element model updating using modal flexibility residual, *Journal of Sound and Vibration***290**(1-2)(2006) 369–387 doi:10.1016/j.jsv.2005.04.006
 25. I. Mekjavić, and D. Domagoj, Damage assessment in bridges based on measured natural frequencies, *International Journal of Structural Stability and Dynamics***17**(2) (2017) 1750022 doi:10.1142/S0219455417500225
 26. Y. Wu, and X. Zhou, L_1 regularized model updating for structural damage detection, *International Journal of Structural Stability and Dynamics***18**(12) (2018) 1850157 doi:10.1142/S0219455418501572
 27. J. Hou, Y. An, S. Wang, Z. Wang, Ł. Jankowski and J. Ou, Structural damage localization and quantification based on additional virtual masses and Bayesian theory, *Journal of Engineering Mechanics***144**(10)(2018) 04018097 doi:10.1061/(asce)em.1943-7889.0001523
 28. A.P. Dempster, Upper and lower probabilities induced by a multi-valued mapping. *The Annals of Mathematical Statistics*,**38** (1967) 325-339 doi:10.1007/978-3-540-44792-4_3
 29. Y. Ding, X. Yao, S. Wang and X. Zhao, Structural damage assessment using improved Dempster-Shafer data fusion algorithm, *Earthquake Engineering and Engineering Vibration***18**(2)(2019) 395–408 doi:10.1007/s11803-019-0511-z
 30. J.P. Sawyer and S.S. Rao, Structural damage detection and identification using fuzzy logic, *AIAA Journal***38**(12)(2000) 2328–2335 doi:10.2514/2.902
 31. Y. Bao, H. Li, Y. An and J. Ou, Dempster-Shafer evidence theory approach to structural damage detection, *Structural Health Monitoring***11**(1)(2012) 13–26 doi:10.1177/1475921710395813
 32. Y. Deng, Generalized evidence theory, *Applied Intelligence***43**(3)(2015) 530–543 doi:10.1007/s10489-015-0661-2
 33. T. Liu, A. Li, Y. Ding, D. Zhao and Z. Li, Multi-source information fusion applied to structural damage diagnosis, *Structure and Infrastructure Engineering***7**(5)(2011) 353–367 doi:10.1080/15732470802588747
 34. X. He, J. Ai and Z. Song, Multi-source data fusion for health monitoring of unmanned aerial vehicle structures, *Applied Mathematics and Mechanics***39**(4)(2018) 395-402 doi:10.21656/1000-0887.380225

J. Hou et al.

35. P. Vanniamparambil, M. Bolhassani, R. Carmi, F. Khan, I. Bartoli, F. Moon, A. Hamid and A. Koutsos, A data fusion approach for progressive damage quantification in reinforced concrete masonry walls, *Smart Materials and Structures* **23**(1)(2013) 015007 doi:10.1088/0964-1726/23/1/015007
36. H. Sun and O. Büyüköztürk, Identification of traffic-induced nodal excitations of truss bridges through heterogeneous data fusion, *Smart Materials and Structures* **24**(7)(2015) 075032 doi:10.1088/0964-1726/24/7/075032
37. E.M. Hernandez, Identification of isolated structural damage from incomplete spectrum information using l_1 -norm minimization, *Mechanical Systems and Signal Processing* **46**(1)(2014) 59–69. doi:10.1016/j.ymsp.2013.12.009
38. J. Juang and R. Pappa, An eigensystem realization algorithm for modal parameter identification and model reduction, *Guidance Control Dynamics* **8**(5)(1985) 620–7 doi:10.2514/3.20031